Excitatory Interactions Between Olfactory Processing Channels in the *Drosophila* Antennal Lobe

Shawn R. Olsen[1], **Vikas Bhandawat**[1], and **Rachel I. Wilson**[*]
Department of Neurobiology, Harvard Medical School, 220 Longwood Ave., Boston MA 02115

Summary

Each odorant receptor gene defines a unique type of olfactory receptor neuron (ORN) and a corresponding type of second-order neuron. Because each odor can activate multiple ORN types, information must ultimately be integrated across these processing channels to form a unified percept. Here we show that, in *Drosophila*, integration begins at the level of second-order projection neurons (PNs). We genetically silence all the ORNs that normally express a particular odorant receptor, and find that PNs postsynaptic to the silent glomerulus receive substantial lateral excitatory input from other glomeruli. Genetically confining odor-evoked ORN input to just one glomerulus reveals that most PNs postsynaptic to other glomeruli receive indirect excitatory input from the single ORN type that is active. Lateral connections between identified glomeruli vary in strength, and this pattern of connections is stereotyped across flies. Thus, a dense network of lateral connections distributes odor-evoked excitation between channels in the first brain region of the olfactory processing stream.

Introduction

All the olfactory receptor neurons (ORNs) that express the same odorant receptor gene respond similarly to odors, and all project to the same sphere of neuropil (glomerulus) in the brain. (Buck, 1996). Furthermore, in most species each second-order olfactory neuron receives direct synaptic input from only one glomerulus. Thus, each odorant receptor gene defines a unique parallel processing channel in the olfactory system.

There is good evidence for cross-talk between these glomerular channels very early in the olfactory system, as early as the level of second-order neurons. Anatomically, glomeruli are interconnected by a network of local interneurons. Functionally, synaptic connections have been demonstrated between interneurons and second-order principal neurons, both in the insect antennal lobe and in the mammalian olfactory bulb (Jahr and Nicoll, 1980;Ernst and Boeckh, 1983;Hoskins et al., 1986;Malun, 1991;Leitch and Laurent, 1996;MacLeod and Laurent, 1996;Stocker et al., 1997;Christensen et al., 1998;Isaacson and Strowbridge, 1998;Python and Stocker, 2002;Urban and Sakmann, 2002;Aungst et al., 2003;Hayar et al., 2004;Wilson et al., 2004;Wilson and Laurent, 2005). It seems likely that these lateral connections have a role in shaping the output of the olfactory bulb and the antennal lobe. However, none of these studies has directly assessed the net effect of glomerular cross-talk on second-order neurons during *in vivo* odor stimulation.

*Correspondence: rachel_wilson@hms.harvard.edu
[1]These authors contributed equally to this work.

Understanding how the antennal lobe and olfactory bulb transform olfactory representations requires an *in vivo* characterization of inter-glomerular synaptic connections. Is the net effect of these lateral connections inhibitory or excitatory? How powerful are these connections compared to direct ORN inputs? How does the amount of lateral input to a second-order neuron vary across odor stimuli? What rules govern the pattern of synaptic connectivity between glomeruli? Is a single glomerulus only connected with glomeruli in its local vicinity? Is each glomerulus only connected to a few others, or is the pattern of connectivity more dense? Is there a correlation between glomerular connectivity and odor tuning? To what extent is the pattern of lateral connectivity stereotyped from one animal to the next?

The most direct way to characterize lateral input to a second-order olfactory neuron would be to silence its direct ORN inputs while preserving ORN input to another glomerulus or glomeruli. Any remaining odor responses in cells postsynaptic to a "silent" glomerulus should reflect purely lateral inputs. This type of experiment is currently not possible in vertebrates, so we have turned to the *Drosophila* antennal lobe. This structure shares the same basic architecture as the vertebrate olfactory bulb, but presents several experimental advantages. First, the odorant receptor gene expressed by most *Drosophila* ORN types has already been identified and mapped onto spatially stereotyped glomeruli in the antennal lobe (Couto et al., 2005;Fishilevich and Vosshall, 2005;Hallem and Carlson, 2006). Second, the circuitry of the *Drosophila* antennal lobe develops properly in the absence of normal olfactory activity, and ORNs target the correct glomerulus even when they do not express a functional receptor (Dobritsa et al., 2003;Berdnik et al., 2006). Finally there are only ~50 glomeruli in the *Drosophila* antennal lobe (as compared to ~1000 in the mouse olfactory bulb) (Laissue et al., 1999). This makes it possible to record from second-order neurons (called projection neurons, or PNs) postsynaptic to an identified ORN input. Importantly, like olfactory bulb mitral cells in most vertebrates, PNs in the *Drosophila* antennal lobe receive direct ORN input from a single glomerulus.

Circumstantial evidence suggests that inter-glomerular connections shape PN odor responses in *Drosophila*. A comparison of odor evoked responses in ORNs and PNs corresponding to the same glomerulus revealed that the rank order of a PN's odor preferences can be different from the preferences of its presynaptic ORNs (Wilson et al., 2004). This argues that a PN's responses are not completely determined by its direct ORN inputs. Instead, it implies that PNs integrate input from multiple ORN types. However, this conclusion has been challenged by functional imaging studies (Ng et al., 2002;Wang et al., 2003).

Here, we use a variety of genetic manipulations and microdissections to remove direct ORN inputs to one or more glomeruli in the *Drosophila* antennal lobe. *In vivo* recordings from PNs postsynaptic to "silent" glomeruli reveal that these PNs receive lateral inputs from other glomeruli. The net effect of lateral synaptic inputs to PNs is predominantly excitatory and can be strong enough to trigger a train of action potentials. In order to define the functional connectivity between identified glomeruli, we have generated flies with only a single active ORN type. Stimulation of just one ORN type is sufficient to recruit lateral excitatory inputs to other glomeruli, but this sensitivity also leads to saturation as more ORN types are activated. A single glomerulus provides indirect excitatory input to most, if not all, glomeruli, thus defining a dense network of lateral connections spanning the entire antennal lobe. However, some lateral excitatory connections are substantially stronger than others. Finally, we find that this pattern of connection strengths is relatively stereotyped across flies, suggesting that it may be genetically hard-wired. These findings directly demonstrate that synaptic cross-talk between glomeruli can shape PN odor responses *in vivo*. Furthermore, our results reveal some of the fundamental rules governing these inter-glomerular interactions.

Results

Olfactory stimuli trigger lateral excitatory interactions among glomeruli

The *Drosophila* antennal lobes receive olfactory input from two peripheral organs, the antennae and the maxillary palps. The palps contain ~120 ORNs which fall into six distinct types not found in the antennae (de Bruyne et al., 1999;Goldman et al., 2005). The antennae contain an additional 43 ORN types not found in the palps (de Bruyne et al., 2001;Hallem et al., 2004). Thus, each glomerulus receives direct ORN input exclusively from either the palps or the antennae. Within the antennal lobe, the six palp glomeruli are intermingled with the 43 antennal glomeruli (Couto et al., 2005;Fishilevich and Vosshall, 2005). This anatomy provides a convenient way to independently manipulate inputs to two groups of glomeruli.

In order to determine whether interactions between glomeruli shape PN odor responses, we began by acutely severing the antennal nerves. This manipulation leaves the palp ORNs intact, and allows us to test whether antennal PNs receive lateral input from palp glomeruli (Fig. 1A). Consistent with previous reports (Berdnik et al., 2006), we found that ablating ORN input to some glomeruli does not induce morphological rearrangement of the remaining ORN axons, even five days post-surgery (Fig. 1B). However, we cannot exclude the possibility that removing ORN input to some glomeruli induces more subtle synaptic plasticity of inter-glomerular connections. Therefore we performed PN recordings immediately after severing the antennal nerves in order to rule out a role for any such plasticity.

Whole-cell patch-clamp recordings from PNs typically show abundant spontaneous synaptic input (Fig. 1C). In contrast, PNs postsynaptic to antennal glomeruli in antennae-less flies show no spontaneous activity (Fig. 1D,E). Nevertheless, odor stimulation of the maxillary palps evokes a depolarization in these PNs (n=6 PNs in 6 flies; Fig. 1D,E). The magnitude of this depolarization varied across cells, but was sufficient to produce a train of spikes in a PN postsynaptic to glomerulus VC3, for example (Fig. 1E). We confirmed that each of the PNs we recorded from innervated an antennal glomerulus by filling the cell with biocytin (see Methods).

We averaged the membrane potential across six presentations of the same odor in the same cell (Fig. 1F) before averaging across experiments (Fig. 1G). All these odors strongly activate one or more palp ORN types (de Bruyne et al., 1999), and all elicited a substantial depolarization in each of the antennal PNs we recorded from. The solvent we use to dilute our odors (paraffin oil) evoked no response (Fig. 1G). Removing both antennae and maxillary palps abolished odor-evoked depolarizations (n = 3), demonstrating that the maxillary palps mediate this response (Fig. 1G).

These results demonstrate that antennal PNs receive lateral synaptic input from palp ORNs, and that the net effect of this indirect input is excitatory. It is possible that some inter-glomerular synapses hyperpolarize PNs, but if so, this inhibition is evidently obscured by a larger excitatory component. It is important to note that ORN input was removed acutely (~10–20 minutes before recording). Therefore, the lateral excitation we observed cannot reflect remodeling of the antennal lobe circuitry.

Total lateral synaptic excitation to a PN is substantial

What is the total impact of all lateral synaptic input to a PN? In order to answer this question we selectively silenced a single ORN type. By recording from PNs postsynaptic to the "silent" glomerulus while stimulating the antennae and palps with odors, we should be able to observe the total lateral input to that PN.

In order to silence a single ORN type, we used flies with mutations in one of two odorant receptor genes, *Or43b* and *Or10a*. *Or43b* is expressed in ORNs that project to glomerulus VM2, and *Or10a* is expressed in ORNs that project to glomerulus DL1 (Couto et al., 2005;Fishilevich and Vosshall, 2005). The *Or43b[1]* null allele was produced by gene targeting, and has been described previously (Elmore et al., 2003). The *Or10a[f03694]* allele results from a pBac insertion in the gene (Thibault et al., 2004), but has not been characterized previously. We first verified that this mutation does not disrupt ORN axon targeting (Supplemental Fig. S1A). We then confirmed that both the *Or43b[1]* and *Or10a[f03694]* mutations virtually abolish ORN odor responses (Supplemental Fig. S1B–D). We occasionally observed very weak responses to a few specific odors in both mutants (Supplemental Fig. S2). These weak responses may be mediated by Or83b, a protein with homology to odorant receptors that is expressed in most ORNs, and which is required for trafficking receptors to the cell membrane (Larsson et al., 2004). We did not use these odors in our stimulus set when we analyzed PN responses in these mutants (Figs. 2–4). Note that these mutations also reduce the rate of spontaneous ORN spikes (Supplemental Fig. S1C).

We then recorded from PNs postsynaptic to these "silent" ORNs (Fig. 2A). In flies with the mutation that silences VM2 ORNs, we targeted VM2 PNs using an enhancer trap line (Tanaka et al., 2004) to specifically label these cells with GFP (*NP5103-Gal4,UAS-CD8:GFP;Or43b[1]*). We recorded from one PN per fly and confirmed the glomerular identity of each recorded PN by imaging the biocytin fill *post hoc*. As expected from the decrease in spontaneous activity in mutant ORNs, spontaneous spiking in VM2 PNs was reduced compared to wild type (Fig. 2B,C). Similarly, in flies with mutant DL1 ORNs, we recorded from DL1 PNs using an enhancer trap line (Tanaka et al., 2004) to specifically label these cells with GFP (*Or10a[f03694];+/+;NP3529-Gal4,UAS-nlsGFP*). Again, spontaneous spiking was reduced in these PNs (Fig. 2B,D). We confirmed that these PNs show normal dendrite morphology in the absence of functional ORNs (Fig. 2C,D), consistent with previous reports (Wong et al., 2002;Berdnik et al., 2006).

In flies with silent VM2 ORNs, all VM2 PNs were depolarized by every odor we tested (*n*=10 cells in 10 flies), with the exception of 4-methyl phenol, which failed to elicit any activity in two cells. These depolarizations were typically large enough to trigger a train of action potentials (Fig. 3). Similarly, in flies with silent DL1 ORNs, all DL1 PNs were depolarized by every odor we tested (*n*=10 cells in 10 flies). Again, most responses were large enough to elicit a train of spikes. We also saw similar spiking responses to odors in cell-attached mode (prior to going whole-cell), demonstrating that these depolarizations are not an artifact of intracellular dialysis.

As expected, most odors evoked a larger response in wild-type flies than in mutant flies. For example, ethyl butyrate elicits vigorous activity in normal VM2 ORNs (Supplemental Fig. S1) and in wild-type VM2 PNs. When the VM2 ORNs are silenced, this odor elicits a much smaller response in VM2 PNs (Fig. 3A1). Similarly, methyl salicylate evokes a very strong response in DL1 ORNs (Supplemental Fig. S1), and in wild-type DL1 PNs, but only a small response in a DL1 PNs postsynaptic to silent ORNs (Fig. 3B1). We also noticed that in PNs postsynaptic to silent ORNs, odor-evoked responses were often more transient than in wild-type PNs (Fig. 3A1,B1).

Some odor responses, however, were relatively unaffected by odorant receptor mutations. For example, 2,3-butanedione evokes very little response in wild-type VM2 ORN (Supplementary Fig. S1). When these ORNs are silenced, the response of VM2 PNs to this odor is virtually unaltered (Fig. 3A2). Similarly, ethyl acetate does not excite wild-type DL1 ORNs (Supplementary Fig. S1). Accordingly, the response of DL1 PNs to ethyl acetate is undiminished by silencing their presynaptic ORNs (Fig. 3B2).

How does the size of total lateral input to a PN depend on the odor stimulus? We quantified odor responses by computing mean firing rates over the 500-ms duration of the odor stimulus, and we plotted these response magnitudes for each odor stimulus to produce tuning curves (Fig. 4A–B). These plots show that different odors evoke different amounts of lateral excitatory input to each PN. However, the odor tuning of PNs postsynaptic to silent ORNs is completely different from the normal odor tuning of these PNs. For both glomeruli, the odor tuning of wild type and mutant PNs showed no significant correlation (both comparisions Pearson's $r^2 < 0.05$, $p > 0.4$).

We also noted that, in the absence of direct ORN inputs, both VM2 PNs and DL1 PNs are broadly tuned to odors. This suggests that each of these glomeruli receives indirect excitatory input from multiple ORN types, not just one or two. We wondered whether these two glomeruli receive indirect input from similar or different populations of ORNs. To assess this, we compared the responses of PNs in these two "silent" glomeruli to the same odors. Overall, the responses of these two PN types are significantly correlated (Fig. 4C; Pearson's $r^2 = 0.31$, $p < 0.05$). However, some odors elicit different amounts of lateral input to these glomeruli. For example, butyric acid elicits a larger response in VM2 than in DL1 ($p = 0.05$, t-test, $n = 6$ for each glomerulus). These results are consistent with the idea that these two glomeruli receive indirect input from overlapping populations of ORNs, but that the indirect inputs to these PNs are not identical.

Characterizing lateral input to many glomeruli originating from a single glomerulus

Because total lateral excitatory input to VM2 and DL1 PNs is broadly tuned and significantly correlated, it is likely that two glomeruli receive indirect input from many of the same ORNs. This, in turn, implies that each ORN type provides indirect input to many glomeruli. To test this prediction directly, we designed experiments to measure the spread of excitation across the antennal lobe evoked by activation of a single ORN type. We used two approaches to selectively stimulate one ORN type (Fig. 5). These two approaches have complementary strengths and weaknesses, but yielded similar results. In the first method (experiment 1), we took advantage of a mutation in *Or83b*. This gene is expressed in most ORNs and encodes a chaperone protein required for trafficking odorant receptors to ORN dendrites (Larsson et al., 2004;Benton et al., 2006). Mutating *Or83b* abolishes odor responses in all maxillary palp ORNs (and many antennal ORNs; Supplemental Fig. S3). Thus, all ORN input to the antennal lobes is abolished by removing the antennae of mutant flies. In these flies, we then rescued normal function in the maxillary palp ORNs that project to glomerulus VA7l. This was done by expressing *Or83b* under the control of the odorant receptor gene promoter corresponding to the VA7l ORNs (*Or46-Gal4/UAS-Or83b;Or83b^2*) (Fishilevich and Vosshall, 2005). We verified the specificity of this rescue by making extracellular ORN recordings from the maxillary palps. Each sensillum in the palp contains exactly two ORNs, and a VA7l ORN is always paired with an ORN that projects to another glomerulus (de Bruyne et al., 1999;Goldman et al., 2005). In the palps of "rescued" flies, we encountered only silent sensilla, or sensilla containing exactly one spontaneously active ORN ($n = 51$ sensilla). This ORN always displayed odor tuning that matched the odor tuning of wild-type VA7l ORNs (Fig 5B, Supplemental Fig. S4). We verified that the rescued ORNs correctly target glomerulus VA7l by co-expressing CD8:GFP with Or83b (Fig. 5C). Furthermore, biocytin fills show that PNs postsynaptic to neighboring glomeruli do not inappropriately invade glomerulus VA7l (Fig. 5C). This argues that the antennal lobe circuitry is grossly normal in the *Or83b^2* mutant.

This approach permits us to selectively stimulate exactly one ORN type. However, it has the drawback that most ORN types are inactive during the development of the fly, which could conceivably produce subtle changes in the antennal lobe circuitry. To address this issue, we used a second method to stimulate one ORN type under conditions in which almost all ORNs

are normal and active throughout the life of the fly; this ensures that normal antennal lobe circuitry is preserved. In this approach (experiment 2, Fig. 5D), we sought to identify a panel of odors that only stimulates one ORN type. Because most ORNs respond to many different odors it is difficult to find such an odor set. To simplify the problem, we cut the antennal nerves just prior to recording, leaving only the six maxillary palp ORN types. Additionally, we used flies bearing the *Δ85* mutation, which abolishes most odor responses in two of the six maxillary palp ORN types (Supplemental Figs. S5 and S6). Thus, in antennae-less flies in a *Δ85* background there are only four functional maxillary palp ORN types. We screened a large panel of odors and identified a set of 14 that exclusively stimulates the VM7 ORNs, while evoking no response from the other three functional ORN types in this genotype. This is demonstrated by local field potential recordings from the maxillary palp. When VM7 ORNs are functional, all odors in this set evoke a local field potential response. These responses are abolished by the $Or42a^{f04305}$ mutation (Thibault et al., 2004), which renders VM7 ORNs nonfunctional (Fig. 5E; see also Supplemental Figs. S5 and S6). In summary, both experiments 1 and 2 permit selective stimulation of one ORN type.

In experiment 1 (genetically rescuing VA71 ORNs), we recorded from a total of 72 PNs postsynaptic to non-rescued glomeruli. PNs were selected at random from the dorsal cluster of PN cell bodies in the antennal lobe. Only one PN was recorded in each fly, which allowed us to unambiguously determine the glomerular identity of each PN after filling it with biocytin. Together, these 72 PNs targeted 24 out of the 49 glomeruli in the antennal lobe. In every one of these PNs, we observed a depolarization while stimulating the VA71 ORNs with odors. This implies that the VA71 ORNs broadcast indirect excitatory input to most glomeruli. As expected, the tuning of the lateral excitatory input to PNs always reflected the tuning of the VA71 ORNs (Fig. 6A). Odors that excited VA71 ORNs produced depolarizations in PNs, whereas inhibition of VA71 ORNs led to a small hyperpolarization. This hyperpolarization probably represents an interruption in tonic lateral excitation driven by spontaneous action potentials in VA71 ORNs.

In experiment 2 (selective odor stimulation of VM7 ORNs), we recorded from a total of 15 PNs. We observed odor-evoked depolarizations in every one of these PNs. This suggests that the VM7 ORNs send lateral excitation indirectly to most glomeruli. And as expected, the tuning of the lateral excitatory input always reflected the tuning of the VM7 ORNs (Fig. 6B). The average magnitude of this depolarization was about half of that observed in experiment 1.

In both experiment 1 (VA71-only) and experiment 2 (VM7-only), the magnitude of lateral depolarization did not scale linearly with ORN firing rate. Odors that evoked only a small ORN response produced a near-maximal lateral depolarization in PNs. Odors that evoked a larger ORN response saturated the lateral circuitry. This is shown by plotting the area under the membrane potential deflection (computed after low-pass filtering the membrane potential) versus ORN firing rate (Fig 6,C,D). The nonlinearity of these curves illustrates both the sensitivity and the saturation of inter-glomerular excitatory circuits. To confirm that the lateral depolarizations in experiment 2 are driven by the VM7 ORNs, we combined the *Δ85* mutation with an odorant receptor gene mutation that silences the VM7 ORNs ($Or42a^{f04305};Δ85$). In this genotype, we saw essentially no odor responses in any PNs (Fig. 6D, open circles, *n*=3).

These results demonstrate that ORN inputs from one glomerular processing channel can easily saturate the lateral excitatory circuitry of the antennal lobe. How are inputs from multiple ORN types integrated by this circuitry? We used an odor blend to investigate how odor-evoked signals from two ORN inputs are combined. In antennae-less *Δ85* flies, the odor 2-butanone (10^{-5} dilution) activates only the VM7 ORNs (Fig. 5E), while the odorant methyl salicylate (10^{-2} dilution) activates only the VA71 ORNs (data not shown). In isolation, these stimuli appear to saturate the lateral excitatory circuitry of the antennal lobe: stimulating VM7 PNs

with 2-butanone evokes a maximal lateral depolarization in experiment 2, and stimulating VA71 PNs with methyl salicylate evokes a maximal lateral depolarization in experiment 1 (Fig. 6, magenta traces). What happens when these two inputs are integrated? When we blended the two odors to stimulate both VA71 and VM7 ORNs simultaneously in antennae-less $\Delta85$ flies, we observed lateral depolarizations that were significantly larger than the response to either odor alone (Fig. 7; p≤0.01 for both comparisons, n=8 PNs, paired t-tests). This shows that multiple ORN inputs are effectively integrated by the lateral excitatory circuitry of the antennal lobe. However, the response to the blend was significantly smaller than that predicted by a linear sum of the responses evoked by stimulating each ORN type individually (Fig 7; $p<10^{-4}$, paired t-test). This demonstrates that saturation occurs across ORN input channels, not just within an ORN input channel.

For a given ORN input (either VA71 or VM7), different PNs showed substantially different amounts of lateral depolarization in response to the same odor. In experiment 1, for example, the response evoked by the strongest odor (4-methyl phenol) ranged from 1.7 mV to 11.8 mV. Responses in some PNs were large enough to elicit a few spikes, but responses in other PNs responses were much weaker. This suggests that different PNs receive different amounts of lateral excitatory input from any given glomerulus. Are these connections random, or are they a stereotyped function of glomerular identity? To address this question, we compared the responses of PNs corresponding to the same glomeruli recorded in different flies. In our data set from experiment 1, there were 11 glomeruli that we hit at least 3 times. In experiment 2, we recorded selectively from PNs in only three glomeruli by using an enhancer trap line to label these cells with GFP (*NP3481-Gal4,UAS-CD8:GFP;+/+;Δ85*). This allowed us to obtain multiple recordings from the same PN type.

Overall, we found that the strength of lateral excitatory connections was relatively stereotyped across flies. In quantitative terms, differences we observed between glomeruli were larger than the variability we observed for a given glomerulus across flies. For example, in experiment 1, selective stimulation of VA71 ORNs produced a significantly greater depolarization in VC4 PNs compared to VA1v PNs (Fig. 8A-C, $p<0.05$; VC4 n=7, VA1v n=8). In experiment 2, selective stimulation of VM7 ORNs produced a significantly greater depolarization in glomerulus DL5 than in glomerulus VM2 or DM6 (Fig 8D-F; $p<0.05$; DL5 n=5, VM2 n=3, DM6 n=7). We also noted that the nonlinear relationship between the lateral depolarization and ORN firing rate had a similar sensitivity and exponential shape across different glomeruli; it is the saturation level that differs (Fig. 8B,E). Together, these results demonstrate that the amount of lateral excitatory input to a PN depends on the identity of the glomerulus where its dendrite is located. The magnitude of lateral depolarization is not correlated with the input resistance of the cell (Pearson's r^2=0.027), ruling out one trivial explanation for this systematic difference.

We next asked whether the magnitude of glomerular cross-talk varied systematically with distance. Figure 9 shows the relative connection strength for all 24 glomeruli we recorded from in experiment 1, mapped in relation to the location of the only glomerulus receiving direct ORN input (VA71). Connection strength is defined as the relative response to 4-methyl phenol, which is the strongest stimulus in our odor set for the VA71 ORNs. This map illustrates that there is no obvious relationship between inter-glomerular distance and the strength of lateral excitatory connections. We also asked if there is a correlation between connection strength and the morphological class of the ORN type corresponding to each glomerulus. Previous studies have shown that ORNs housed in the three major morphological classes of sensilla (basiconic, coeloconic, and trichoid) tend to project to nearby glomeruli and therefore define several zones in the antennal lobe (Couto et al., 2005;Fishilevich and Vosshall, 2005). Fig. 9B shows that the zones defined by these sensillum classes receive similar overall levels of lateral excitation. Finally, we tested whether there is a relationship between the odor tuning of the normal ORN

input to a glomerulus and the strength of excitatory lateral input it receives from VA71. Comprehensive odor tuning data for 16 of the colored glomeruli in Fig. 9A has been compiled by other investigators (Hallem and Carlson, 2006). We used this data set to compute the correlation coefficient (Pearson's *r*) between ORN odor responses for every pair-wise combination of these 16 glomeruli, and then plotted the difference in lateral depolarization for each pair as a function of this correlation. We found there is no relationship between glomerular tuning and depolarization strength (Fig. 9C).

Discussion

In this study, our goal was to observe the synaptic inputs to PNs arising from local antennal lobe circuits. We have used a variety of complementary strategies to remove direct ORN input to the PN we were recording from, meanwhile leaving other ORNs intact. These manipulations allowed us to directly observe lateral excitatory input to a PN originating from other glomeruli.

It is important to emphasize that this lateral excitation cannot be ascribed purely to compensatory rearrangement of the antennal lobe circuitry. This point is most forcefully demonstrated by experiments in which most or all ORNs are normal and active until we sever the antennal nerves immediately before recording (Fig. 1, Fig. 6B). In these experiments we recorded from PNs 10–20 minutes after removing the antennae and always observed odor-evoked lateral depolarizations. Hence, the circuitry mediating these responses must exist in normal flies prior to removing antennal input.

An individual PN integrates lateral inputs from many ORN types

Excitatory connections between glomeruli appear to be very dense, perhaps all-to-all. This conclusion is supported by four pieces of evidence. First, the magnitude of the depolarization we observed when almost all ORNs are intact (Figs. 2–4) is larger than that observed when only the maxillary palp ORNs are intact (Fig. 1), which in turn is larger than that observed when only a single ORN type is intact (Figs. 5–9). This argues that most PNs receive indirect input from many ORN types. Second, when we restricted ORN input to a single glomerulus, every PN we recorded from (87 of 87 cells) received at least weak lateral input from that glomerulus. This implies that each ORN type broadcasts indirect input to most or all glomeruli. Third, the odor tuning of the total lateral input to a glomerulus is much broader than the odor tuning of a typical ORN. Fourth, the lateral input to VM2 PNs and DL1 PNs has a relatively similar (though not identical) odor tuning profile. This suggests that large and overlapping populations of ORNs provide indirect input to these two types of PNs. All-to-all connectivity is a parsimonious explanation for all these observations.

A specific matrix of excitatory connections

It should be noted that although lateral excitatory connectivity is dense, and perhaps all-to-all, it is nevertheless selective. When we stimulated a single ORN type and recorded sequentially from PNs in different glomeruli, we found that each PN type receives a characteristically strong or weak lateral input from that ORN type. Furthermore, these characteristic connection strengths are relatively stereotyped across flies. This suggests that the synaptic connectivity of local interneurons in the antennal lobe may be genetically hardwired.

Notably, the strength of these lateral excitatory connections is not correlated with the distance between the target glomerulus and the location of the ORN inputs. This means that the spatial relationship between glomeruli does not limit the strength of their lateral interactions. This finding also argues that lateral excitation does not reflect spillover of excitatory neurotransmitter from the glomerulus receiving active ORN input, since in this case PNs closer to the active glomerulus would be expected to see a larger depolarization.

There is some tension between the idea that excitatory connection strengths between glomeruli are varied, and the finding that VM2 and DL1 PNs see similarly-tuned total lateral excitatory input. One possibility is that the lateral inputs to VM2 and DL1 PNs just happen to be unusually well-correlated. Another possibility is that a given target glomerulus receives characteristically strong (or characteristically weak) indirect inputs from all ORN types. In this latter scenario, the strength of the lateral depolarization would vary across glomeruli, but its odor tuning would not.

Sensitivity and saturation of lateral excitatory circuits

The lateral excitatory circuits of the antennal lobe are remarkably sensitive to small levels of afferent input. We have shown that activating ORNs presynaptic to a single glomerulus produces a substantial lateral depolarization in many or all PNs. Moreover, the magnitude of the lateral depolarization arising from a single ORN type is extremely sensitive to small increases in ORN firing rate. Even an odor that evokes a very weak response in these ORNs (e.g., 1-butanol or geranyl acetate in Fig. 6) still evokes substantial lateral excitation.

Another striking feature of lateral excitatory circuits is their saturability. In experiments where we stimulated only one ORN type, increasing the rate of incoming ORN spikes from 50 to 150 spikes/second had little effect on the amount of lateral excitatory input that was broadcast to other glomeruli. Furthermore, in experiments where we stimulated two ORN types, the combined effect of these two input channels was substantially less than the sum of each channel when stimulated individually. This type of saturation should tend to limit the magnitude of lateral excitatory synaptic input to a PN.

Together, these results suggest that the impact of lateral excitatory connections might be strongly dependent on odor concentration. Testing this hypothesis will require comparing the sensitivity of direct and lateral inputs to a range of concentrations, and understanding how these inputs are integrated by PNs.

A cellular substrate for lateral excitatory connections

While this manuscript was under review, a report appeared that identified a novel population of cholinergic local neurons in the *Drosophila* antennal lobe (Shang et al., 2007). There is no direct evidence that these local neurons mediate the local excitatory connections we have observed, but this hypothesis seems plausible. Each cholinergic local neuron reportedly innervates most glomeruli, and this morphology could easily explain our observation that a single ORN type broadcasts excitatory input to most or all PNs. Interestingly, excitatory (glutamatergic) local neurons were also recently identified in the olfactory bulb (Aungst et al., 2003), although it is not known whether these cells make synapses onto mitral cells, the analog of antennal lobe PNs.

Shang et al. also independently provided evidence that PNs receive lateral excitatory input. As in our study (Figs. 2–4), these investigators measured activity in PNs whose presynaptic ORNs have been silenced by an odorant receptor gene mutation. Complementary to our electrophysiological approach, Shang et al. used a genetically-encoded ecliptic pHluorin to monitor the balance of synaptic vesicle exocytosis and endocytosis at presynaptic sites in PN dendrites. They found that PNs whose presynaptic ORNs were silent still showed odor-evoked dendritic synaptopHluorin signals, implying that these PNs receive indirect excitatory input from other ORNs.

Lateral inhibition in the *Drosophila* antennal lobe

Models of olfactory processing in the insect antennal lobe and the vertebrate olfactory bulb stress the importance of inhibitory connections between glomeruli (Mori et al., 1999;Laurent,

2002). What about lateral inhibition in the *Drosophila* antennal lobe? It is known that GABAergic interneurons ramify throughout the *Drosophila* antennal lobe and release GABA in response to odor stimulation (Stocker et al., 1997;Ng et al., 2002;Wilson and Laurent, 2005). *Drosophila* antennal lobe PNs have $GABA_A$-like and $GABA_B$-like receptors, and antagonists of these receptors disinhibit PN odor responses (Wilson and Laurent, 2005). Given this, it is perhaps surprising that we have not observed lateral synaptic inhibition in PNs.

Several considerations put this finding in perspective. First, although the lateral inputs we observe are dominated by excitation, it is possible that these responses reflect the integration of both excitatory and inhibitory inputs. As a result, inhibition could be masked by a larger postsynaptic excitation. Second, although our results are inconsistent with a dominant role for inter-glomerular postsynaptic inhibition of PNs, our findings do not preclude a role for inter-glomerular presynaptic inhibition of ORN axon terminals. Presynaptic inhibition of neurotransmitter release from ORN axons is a well-known phenomenon in the mammalian olfactory bulb (Ennis et al., 2001;McGann et al., 2005;Murphy et al., 2005;Wachowiak et al., 2005) and in the crustacean olfactory lobe (Wachowiak et al., 2002). In this study, we abolished or severely reduced direct ORN input to the PNs we were recording from, which necessarily prevents us from observing any substantial presynaptic inhibition.

It is worth noting that neither $GABA_A$ nor $GABA_B$ receptors can mediate the lateral depolarization we observe. Both $GABA_A$ and $GABA_B$ conductances are hyperpolarizing in PNs (Wilson and Laurent, 2005). And although $GABA_A$ and $GABA_B$ receptor antagonists together completely block GABA-evoked hyperpolarizations in PNs (Wilson and Laurent, 2005), they do not diminish the lateral depolarization we describe in this study (Supplemental Fig. S7). This result also demonstrates that the lateral depolarization does not represent disinhibition (inhibition of inhibitory input to PNs).

Implications of lateral excitatory connections for odor processing

A significant transformation in odor responses occurs between the ORN and PN layer in the *Drosophila* olfactory system. First, the odor tuning of PNs can be broader than the odor tuning of their presynaptic ORNs (Wilson et al., 2004). This may reflect, in part, the effects of the lateral excitatory connections we have described in this study. Because we have observed that the odor tuning of lateral input to a PN is different from the odor tuning of its direct ORN input, it seems likely that these lateral inputs promote excitatory responses to odors that would not have otherwise excited that PN. A second feature of the ORN-to-PN transformation is that the rank order of PN odor preferences can differ from the odor preferences of their presynaptic ORNs (Wilson et al., 2004). Again, because the odor tuning of lateral input to a PN is different from the odor tuning of its direct ORN input, it seems likely that lateral excitatory connections between glomeruli contribute to this phenomenon.

However, it would be misleading to neatly assign different components of a PN's odor response to direct versus lateral excitatory inputs. Direct and lateral excitation may co-exist with pre- and postsynaptic inhibition, and all these inputs are likely to be integrated by PNs in a nonlinear fashion. Broad tuning in PNs could also reflect some nonlinearity in ORN-to-PN connections.

In general, bridging the gap between cellular and systems neuroscience will require a deeper understanding of how neurons integrate complex synaptic inputs *in vivo*. Using a combination of genetic techniques and *in vivo* electrophysiology, we have begun to dissect the various synaptic interactions involved in odor processing in the *Drosophila* antennal lobe. Our strategy has been to eliminate one input to an identified neuron in order to unmask other relevant interactions. Here this approach has revealed broadly distributed but specific excitatory connections between glomeruli. Although the behavior of a neural circuit is ultimately a complex product of its components, some insight can nevertheless be gained by manipulating

one element at a time, provided that appropriate genetic tools are available. In this respect, the *Drosophila* olfactory circuit represent a powerful system for understanding the synaptic and cellular computations performed on sensory stimuli that ultimately produce perception and behavior.

Experimental procedures

Fly stocks

Flies were reared at room temperature on conventional cornmeal agar. All experiments were performed on adult female flies 2–7 days post-eclosion. Fly stocks were kindly provided as follows: *Or10a-Gal4* (Barry Dickson); *Or43b[1]* (Dean Smith); *NP5103-Gal4*, *NP3529-Gal4*, and *NP3481-Gal4* (Kei Ito and Liqun Luo); *UAS-Or83b*, *Or83b-Gal4*, *Or83b[2]*, *Or46a-Gal4*, *Or92a-Gal4*, and *Or42b-Gal4* (Leslie Vosshall); *UAS-DTl/CyO* and *UAS-DTl$_{III}$* (Leslie Stevens). UAS-CD8:GFP$_I$, UAS-CD8:GFP$_{II}$, and UAS-CD8:GFP$_{III}$ were obtained from the Bloomington Stock Center. *Or10a^{f03694}* and *Or42a^{f04305}* are indexed on Flybase as pBac insertions and were obtained from Bloomington. We found that the *Or42a^{f04305}* stock had a second mutation that specifically affects the pb2A and pb3B neurons (Supplemental Figs. S5–S6). This mutation is on the third chromosome and most likely affects the odorant receptor genes *Or85e* and *Or85d*, which are expressed in the pb2A and pb3B neurons, respectively. We term this mutation *Δ85*. The *Or42a^{f04305}* and *Δ85* mutations were separated using standard genetic crosses. The genotypes used in all experiments are listed in Supplementary Table S1.

ORN recordings

Flies were immobilized in the trimmed end of a plastic pipette tip. A reference electrode filled with *Drosophila* saline was inserted into the eye, and a sharp saline-filled glass capillary (tip diameter < 1µm) was inserted into a sensillum. Sensilla were visualized using an Olympus BX51WI microscope with a 50x air objective. Sensillum types were identified based on their morphology and their characteristic responses to a panel of odors (de Bruyne et al., 1999;de Bruyne et al., 2001). For recordings from flies with rescued VA7l ORNs we recorded semi-randomly from all three types of sensilla on the maxillary palp (pb2 sensilla which contain the VA7l ORNs are slightly thinner than pb1 and pb3, which allowed us to bias our recordings toward pb2). Voltage signals were acquired with an A-M Systems Model 2400 amplifier (10MΩ headstage). Signals were low-pass filtered at 2kHz and digitized at 10kHz. ORN spikes were detected off-line using routines in IgorPro (Wavemetrics). In all cases except ab1 sensilla, spikes could be easily sorted based on their different shapes. In the case of ab1 sensilla there are four neurons and hence four kinds of spikes, of which the DL1 ORN spikes are the smallest. To get accurate estimates for the response of the DL1 ORNs to some odors, we needed to kill other neurons in this sensillum (see Supplemental Table S1). Due to genetic constraints, this was not done for the mutant DL1 ORNs. Hence, responses to some odors that activate the other neurons in this sensillum strongly could not be determined, and are marked (‡) in Supplemental Fig. S1. Local field potentials were recorded with an electrode inserted into the antenna or maxillary palp, and a reference electrode in the eye.

PN recordings

Whole-cell recordings from PNs were performed *in vivo* as previously described (Wilson and Laurent, 2005). For some experiments the antennal nerves were severed with fine forceps just prior to recording. The composition of the internal patch-pipette solution was (in mM): potassium aspartate 140, HEPES 10, MgATP 4, Na$_3$GTP 0.5, EGTA 1, KCl 1, biocytin hydrazide 13 (pH = 7.3, osmolarity adjusted to ~ 265 mOsm). The composition of the external saline solution was (in mM): NaCl 103, *N*-tris(hydroxymethyl) methyl-2-aminoethane-sulfonic acid 5, trehalose 8, glucose 10, NaHCO$_3$ 26, NaH$_2$PO$_4$ 1, CaCl$_2$, and MgCl$_2$ 1.5. Osmolarity was adjusted to 270–275 mOsm. The saline was bubbled with 95% O$_2$/5% CO$_2$

and reached a final pH = 7.3. Voltage recordings were obtained with an A-M Systems Model 2400 amplifier in the current clamp mode (10Ω headstage). Signals were low-pass filtered at 5kHz and digitized at 10kHz. An Olympus BX51WI microscope with a 40x water-immersion objective, IR-DIC optics, and a fluorescence attachment was used to obtain recordings under visual control. One neuron was recorded per brain and the morphology of each cell was visualized *post hoc* with biocytin histochemistry. Histochemistry with biocytin-streptavidin and nc82 antibody was performed as described previously (Wilson and Laurent, 2005), except that in the secondary incubation we used 1:250 goat anti-mouse:AlexaFluor633 and 1:1000 streptavidin:AlexaFluor568 (Molecular Probes). The nc82 antibody (used to outline glomerular boundaries) was obtained from the Developmental Studies Hybridoma Bank (U. of Iowa). Histochemistry with α-CD8 antibody (Figs. 1B,5C, and Supplemental S1A) was performed as described previously (Wilson and Laurent, 2005). Glomeruli were identified using published maps (Laissue et al., 1999;Couto et al., 2005).

Olfactory stimulation

Odors were diluted in paraffin oil at a ratio of 1:100 (except for the VM7-only experiments, see below). Odors in Figs. 4 are benzaldehyde (BNZ), butyric acid (BUA), 2,3-butanedione (BUD), 1-butanol (BUT), cyclohexanone (CYH), cis-3-hexen-1-ol (CIS), ethyl butyrate (EBA), ethyl acetate (ETA), geranyl acetate (GER), methyl salicylate (MSL), 3-methylthio-1-propanol (MTP), 4-methyl phenol (MPH), γ-valerolactone (VAL). Odors used for stimulation of rescued VA71 ORNs (Fig. 6A,C; Fig. 8A–C; Fig. 9) were 4-methyl phenol, benzaldehyde, methyl salicylate, ethyl acetate, 1-butanol, cyclohexanone, 3-octanol, and paraffin oil. For selective stimulation of VM7 ORNs (Fig. 5E; Fig. 6B,D; Fig. 7A; Fig. 8D–F), dilution ratios in paraffin oil were adjusted for most odors to achieve specific stimulation; odors were acetone (10^{-4} dilution), 2-butanone (10^{-5}), ethyl acetate (10^{-4}), geranyl acetate (10^{-3}), hexanal (10^{-4}), hexyl acetate (10^{-4}), isoamyl acetate (10^{-6}), methyl acetate (10^{-4}), octanal (10^{-4}), propanal (10^{-4}), 2-pentanone (10^{-4}), trans-2-hexenal (10^{-4}), butyric acid (10^{-2}), and paraffin oil. Odor source details are at http://wilson.med.harvard.edu/odors.html. Odors were delivered with a custom-built olfactometer. A continuous stream of charcoal-filtered air (2.2 L/min) was directed over the fly. Switching of a 3-way solenoid redirected 200 mL/min of this air through an odor vial, which rejoined the air stream 12 cm from the end of the odor tube. Thus, all odors were diluted 10-fold in air just before reaching the fly. All odor stimuli were applied for 500 msec. The odor tube was ~8 mm in diameter and terminated ~8 mm from the fly.

Data analysis

Data were analyzed using custom software written in Igor Pro (Wavemetrics). In Figs. 1, 6, 7, and 8, PN voltage traces were averaged over six repeated presentations of each odor and low-pass filtered offline at 13Hz to remove spikes before averaging across experiments. Depolarization area was computed as the area under the zeroed membrane potential over a 500-ms window starting 100 ms after opening of the odor valve. Traces are presented as the mean ± SEM across experiments. Tuning curves in Fig. 4 were generated by computing mean firing rate over the 500-ms odor presentation, minus the baseline firing rate.

Supplementary Material

Refer to Web version on PubMed Central for supplementary material.

References

Aungst JL, Heyward PM, Puche AC, Karnup SV, Hayar A, Szabo G, Shipley MT. Centre-surround inhibition among olfactory bulb glomeruli. Nature 2003;426:623–629. [PubMed: 14668854]

Benton R, Sachse S, Michnick SW, Vosshall LB. Atypical membrane topology and heteromeric function of Drosophila odorant receptors in vivo. PLoS Biol 2006;4:e20. [PubMed: 16402857]

Berdnik D, Chihara T, Couto A, Luo L. Wiring stability of the adult Drosophila olfactory circuit after lesion. J Neurosci 2006;26:3367–3376. [PubMed: 16571743]

Buck LB. Information coding in the vertebrate olfactory system. Annu Rev Neurosci 1996;19:517–544. [PubMed: 8833453]

Christensen TA, Waldrop BR, Hildebrand JG. Multitasking in the olfactory system: context-dependent responses to odors reveal dual GABA-regulated coding mechanisms in single olfactory projection neurons. J Neurosci 1998;18:5999–6008. [PubMed: 9671685]

Couto A, Alenius M, Dickson BJ. Molecular, anatomical, and functional organization of the Drosophila olfactory system. Curr Biol 2005;15:1535–1547. [PubMed: 16139208]

de Bruyne M, Clyne PJ, Carlson JR. Odor coding in a model olfactory organ: the Drosophila maxillary palp. J Neurosci 1999;19:4520–4532. [PubMed: 10341252]

de Bruyne M, Foster K, Carlson JR. Odor coding in the Drosophila antenna. Neuron 2001;30:537–552. [PubMed: 11395013]

Dobritsa AA, van der Goes van Naters W, Warr CG, Steinbrecht RA, Carlson JR. Integrating the molecular and cellular basis of odor coding in the Drosophila antenna. Neuron 2003;37:827–841. [PubMed: 12628173]

Elmore T, Ignell R, Carlson JR, Smith DP. Targeted mutation of a Drosophila odor receptor defines receptor requirement in a novel class of sensillum. J Neurosci 2003;23:9906–9912. [PubMed: 14586020]

Ennis M, Zhou FM, Ciombor KJ, Aroniadou-Anderjaska V, Hayar A, Borrelli E, Zimmer LA, Margolis F, Shipley MT. Dopamine D2 receptor-mediated presynaptic inhibition of olfactory nerve terminals. J Neurophysiol 2001;86:2986–2997. [PubMed: 11731555]

Ernst KD, Boeckh J. A neuroanatomical study on the organization of the central antennal pathways in insects. III. Neuroanatomical characterization of physiologically defined response types of deutocerebral neurons in Periplaneta americana. Cell Tissue Res 1983;229:1–22. [PubMed: 6831538]

Fishilevich E, Vosshall LB. Genetic and functional subdivision of the Drosophila antennal lobe. Curr Biol 2005;15:1548–1553. [PubMed: 16139209]

Goldman AL, van der Goes van Naters W, Lessing D, Warr CG, Carlson JR. Coexpression of two functional odor receptors in one neuron. Neuron 2005;45:661–666. [PubMed: 15748842]

Hallem EA, Carlson JR. Coding of odors by a receptor repertoire. Cell 2006;125:143–160. [PubMed: 16615896]

Hallem EA, Ho MG, Carlson JR. The molecular basis of odor coding in the Drosophila antenna. Cell 2004;117:965–979. [PubMed: 15210116]

Hayar A, Karnup S, Ennis M, Shipley MT. External tufted cells: a major excitatory element that coordinates glomerular activity. J Neurosci 2004;24:6676–6685. [PubMed: 15282270]

Hoskins SG, Homberg U, Kingan TG, Christensen TA, Hildebrand JG. Immunocytochemistry of GABA in the antennal lobes of the sphinx moth Manduca sexta. Cell Tissue Res 1986;244:243–252. [PubMed: 3521878]

Isaacson JS, Strowbridge BW. Olfactory reciprocal synapses: dendritic signaling in the CNS. Neuron 1998;20:749–761. [PubMed: 9581766]

Jahr CE, Nicoll RA. Dendrodendritic inhibition: demonstration with intracellular recording. Science 1980;207:1473–1475. [PubMed: 7361098]

Laissue PP, Reiter C, Hiesinger PR, Halter S, Fischbach KF, Stocker RF. Three-dimensional reconstruction of the antennal lobe in Drosophila melanogaster. J Comp Neurol 1999;405:543–552. [PubMed: 10098944]

Larsson MC, Domingos AI, Jones WD, Chiappe ME, Amrein H, Vosshall LB. Or83b encodes a broadly expressed odorant receptor essential for Drosophila olfaction. Neuron 2004;43:703–714. [PubMed: 15339651]

Laurent G. Olfactory network dynamics and the coding of multidimensional signals. Nat Rev Neurosci 2002;3:884–895. [PubMed: 12415296]

Leitch B, Laurent G. GABAergic synapses in the antennal lobe and mushroom body of the locust olfactory system. J Comp Neurol 1996;372:487–514. [PubMed: 8876449]

MacLeod K, Laurent G. Distinct mechanisms for synchronization and temporal patterning of odor-encoding neural assemblies. Science 1996;274:976–979. [PubMed: 8875938]

Malun D. Synaptic relationships between GABA-immunoreactive neurons and an identified uniglomerular projection neuron in the antennal lobe of Periplaneta americana: a double-labeling electron microscopic study. Histochemistry 1991;96:197–207. [PubMed: 1917576]

McGann JP, Pirez N, Gainey MA, Muratore C, Elias AS, Wachowiak M. Odorant representations are modulated by intra- but not interglomerular presynaptic inhibition of olfactory sensory neurons. Neuron 2005;48:1039–1053. [PubMed: 16364906]

Mori K, Nagao H, Yoshihara Y. The olfactory bulb: coding and processing of odor molecule information. Science 1999;286:711–715. [PubMed: 10531048]

Murphy GJ, Darcy DP, Isaacson JS. Intraglomerular inhibition: signaling mechanisms of an olfactory microcircuit. Nat Neurosci 2005;8:354–364. [PubMed: 15696160]

Ng M, Roorda RD, Lima SQ, Zemelman BV, Morcillo P, Miesenbock G. Transmission of olfactory information between three populations of neurons in the antennal lobe of the fly. Neuron 2002;36:463–474. [PubMed: 12408848]

Python F, Stocker RF. Immunoreactivity against choline acetyltransferase, gamma-aminobutyric acid, histamine, octopamine, and serotonin in the larval chemosensory system of Drosophila melanogaster. J Comp Neurol 2002;453:157–167. [PubMed: 12373781]

Shang Y, Claridge-Chang A, Sjulson L, Pypaert M, Miesenbock G. Excitatory local circuits and their implications for olfactory processing in the fly antennal lobe. Cell 2007;128:601–612. [PubMed: 17289577]

Stocker RF, Heimbeck G, Gendre N, de Belle JS. Neuroblast ablation in Drosophila P[GAL4] lines reveals origins of olfactory interneurons. J Neurobiol 1997;32:443–456. [PubMed: 9110257]

Tanaka NK, Awasaki T, Shimada T, Ito K. Integration of chemosensory pathways in the Drosophila second-order olfactory centers. Curr Biol 2004;14:449–457. [PubMed: 15043809]

Thibault ST, Singer MA, Miyazaki WY, Milash B, Dompe NA, Singh CM, Buchholz R, Demsky M, Fawcett R, Francis-Lang HL, et al. A complementary transposon tool kit for Drosophila melanogaster using P and piggyBac. Nat Genet 2004;36:283–287. [PubMed: 14981521]

Urban NN, Sakmann B. Reciprocal intraglomerular excitation and intra- and interglomerular lateral inhibition between mouse olfactory bulb mitral cells. J Physiol 2002;542:355–367. [PubMed: 12122137]

Wachowiak M, Cohen LB, Ache BW. Presynaptic inhibition of olfactory receptor neurons in crustaceans. Microsc Res Tech 2002;58:365–375. [PubMed: 12214303]

Wachowiak M, McGann JP, Heyward PM, Shao Z, Puche AC, Shipley MT. Inhibition of olfactory receptor neuron input to olfactory bulb glomeruli mediated by suppression of presynaptic calcium influx. J Neurophysiol 2005;94:2700–2712. [PubMed: 15917320]

Wang JW, Wong AM, Flores J, Vosshall LB, Axel R. Two-photon calcium imaging reveals an odor-evoked map of activity in the fly brain. Cell 2003;112:271–282. [PubMed: 12553914]

Wilson RI, Laurent G. Role of GABAergic inhibition in shaping odor-evoked spatiotemporal patterns in the Drosophila antennal lobe. J Neurosci 2005;25:9069–9079. [PubMed: 16207866]

Wilson RI, Turner GC, Laurent G. Transformation of olfactory representations in the Drosophila antennal lobe. Science 2004;303:366–370. [PubMed: 14684826]

Wong AM, Wang JW, Axel R. Spatial representation of the glomerular map in the Drosophila protocerebrum. Cell 2002;109:229–241. [PubMed: 12007409]
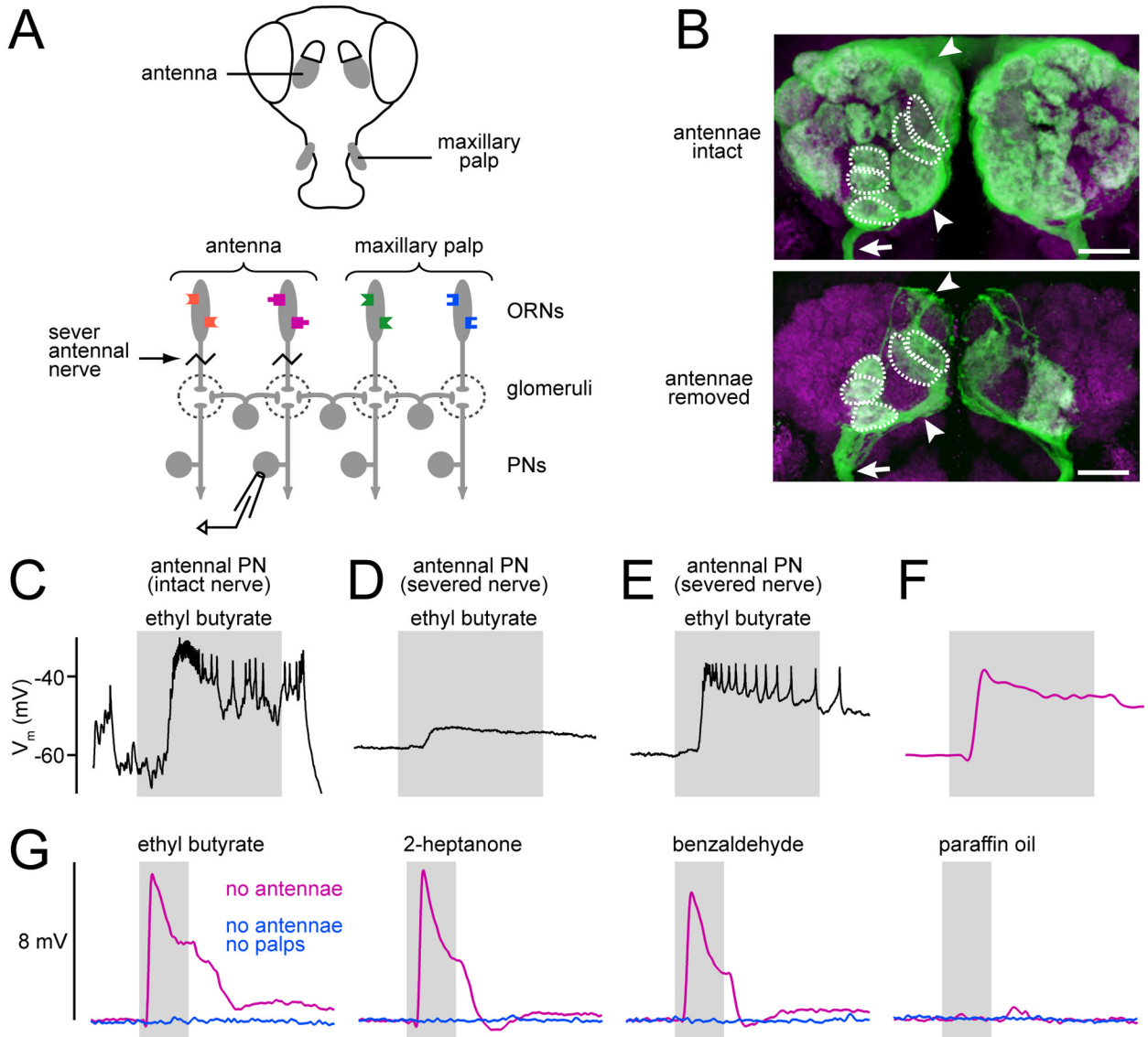
Figure 1. Olfactory stimuli trigger excitatory interactions among glomeruli

(A) Both the antennae and the maxillary palps project to the antennal lobes. Severing the antennal nerves removes direct ORN input to antennal glomeruli, but leaves input to palp glomeruli intact. Recording from a PN postsynaptic to a deafferented glomerulus reveals indirect input to that cell from palp ORNs.

(B) Axon targeting of palp ORNs is not altered by removing antennal ORNs. Projections of confocal stacks through the antennal lobes (neuropil in magenta) show ORN axons labeled with CD8:GFP (green). Glomeruli targeted by palp ORNs are outlined. Arrow indicates maxillary nerve. Arrowheads indicate axons projecting to or from the midline; each ORN projects bilaterally. Scale bars=20 μm.

(C) With antennal nerve intact, a recording from an antennal PN (in glomerulus DM3) shows spontaneous and odor-evoked activity. Period of odor delivery is indicated by gray bar (500 msec).

(D) Recording from an antennal PN (in glomerulus DM3) after severing antennal nerves. Spontaneous activity is abolished, but a small odor-evoked depolarization remains.

(E) Recording from an antennal PN (in glomerulus VC3) after severing antennal nerves shows a large odor-evoked depolarization.

(F) Same as E, but averaged across 6 trials with the same odor, and low-pass filtered to remove spikes.

(G) Odor-evoked depolarizations averaged across all experiments with severed antennal nerves (magenta). No depolarization is observed when both antennae and maxillary palps are removed (blue). Note that this analysis pools data from 6 PNs corresponding to different antennal glomeruli.
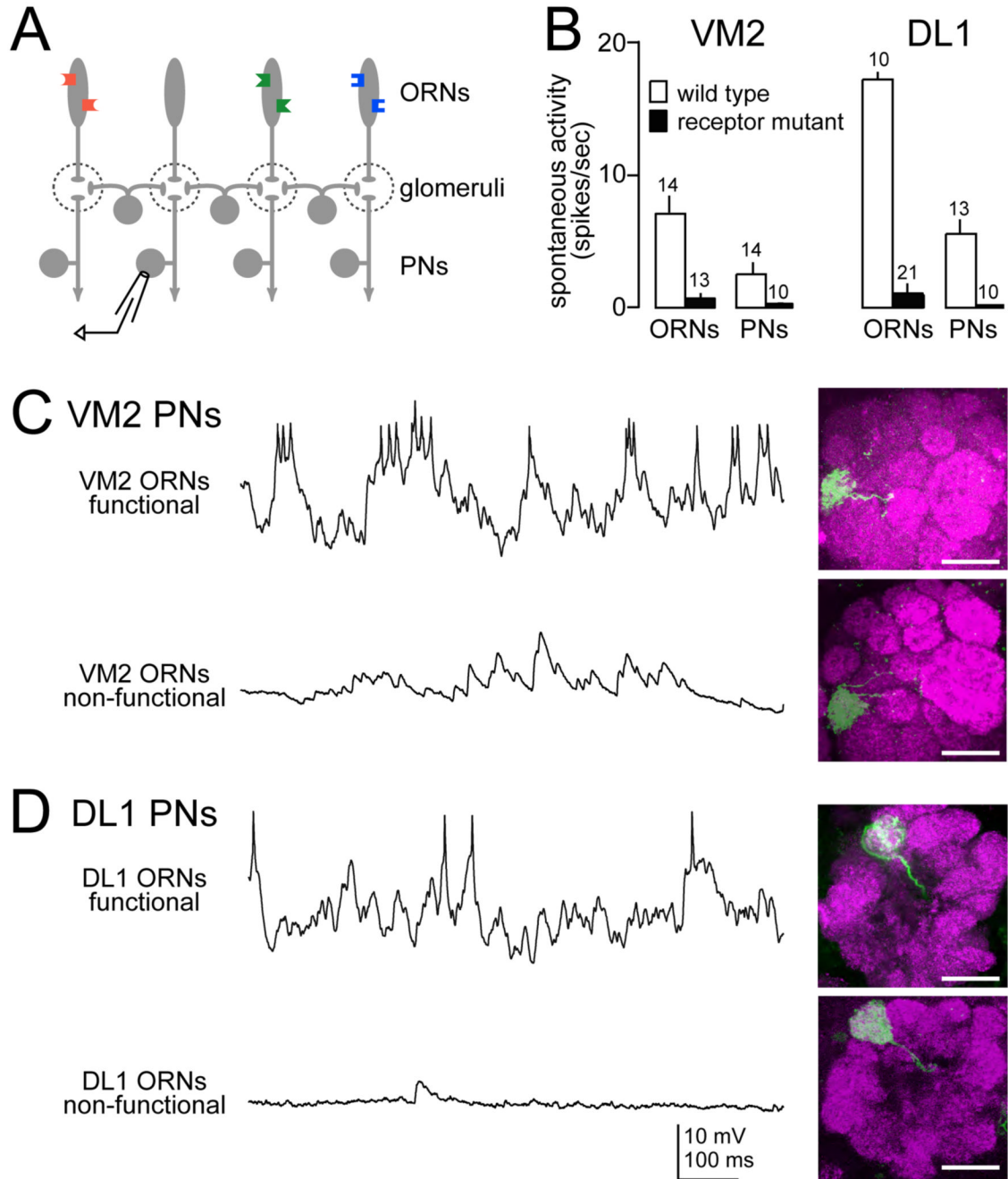
Figure 2. PNs postsynaptic to "silent" ORNs show reduced activity but normal morphology

(A) Schematic of experiments in Figs. 2–4: recording from PNs postsynaptic to ORNs lacking odorant receptors.

(B) Odorant receptor mutations reduce spontaneous activity in both ORNs and their postsynaptic PNs. Bars show mean ± SEM averaged across experiments, with *n* values above each bar ($p<0.05$ for each wild type/mutant comparison, t-tests).

(C) Spontaneous electrophysiological activity and morphology of VM2 PNs in wild-type flies (top) and *Or43b[1]* mutant flies (bottom). Images on the right are projections of confocal stacks through one antennal lobe (neuropil in magenta) showing the primary dendrite of the biocytin-

filled PN (biocytin/streptavidin in green). The cell body and axon of the recorded PN are not present in these *z*-sections. Scale bars=20 μm.

(D) Spontaneous electrophysiological activity and morphology of DL1 PNs in wild-type flies (top) and *Or10a^{f03694}* mutant flies (bottom).
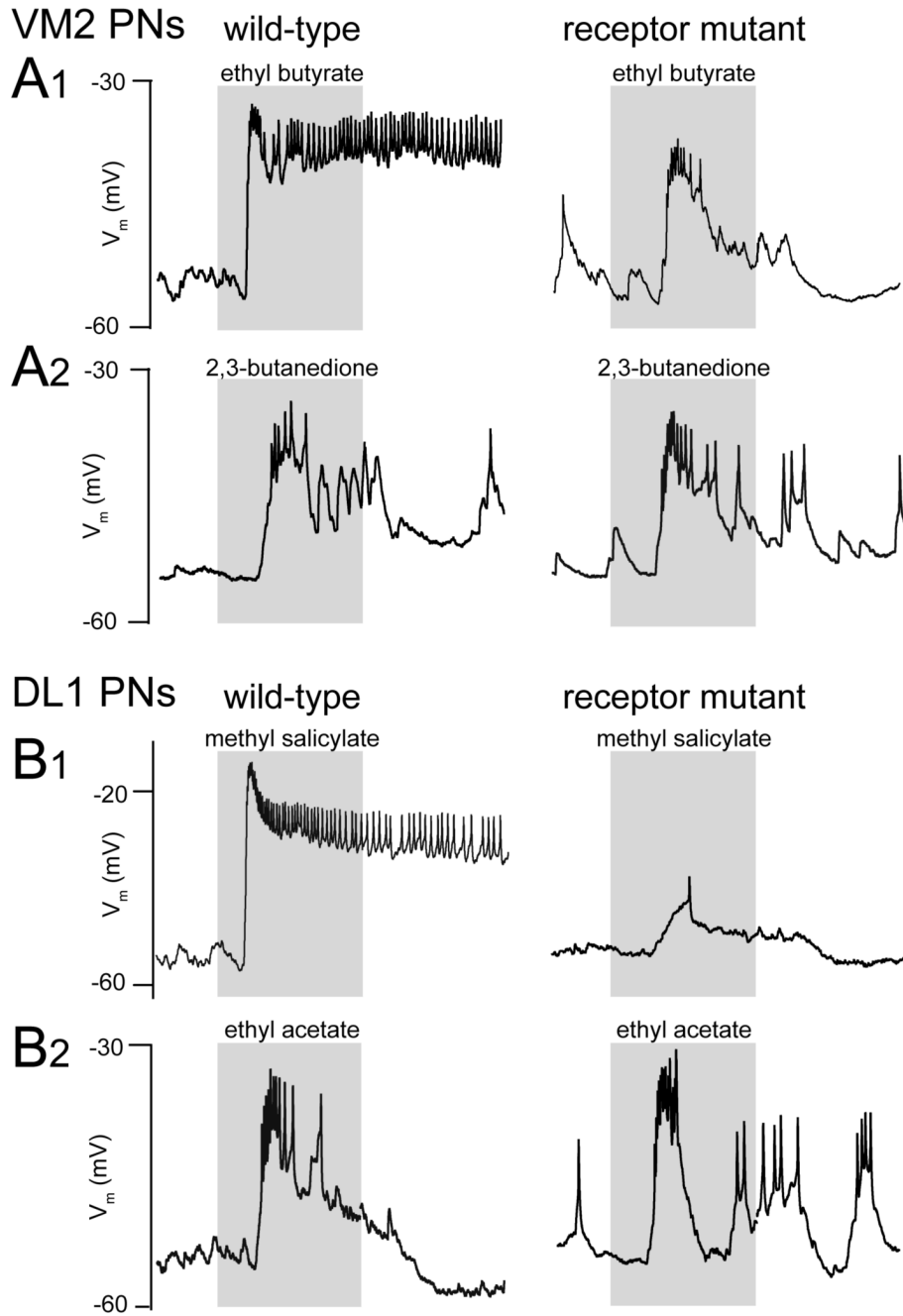
Figure 3. Comparing odor responses in PNs postsynaptic to normal versus "silent" ORNs
Representative responses of PNs postsynaptic to wild-type ORNs (left column) and PNs postsynaptic to non-functional ORNs (right column). Most odors elicit a substantially larger response when presynaptic ORNs are functional (A1, B1). However, some odors elicit a similar response with or without functional presynaptic ORNs (A2, B2). Gray bars indicate the 500-ms period of odor stimulation. Transient stimulus artifacts from the olfactometer (at the end of the odor stimulus period) were blanked in some traces.
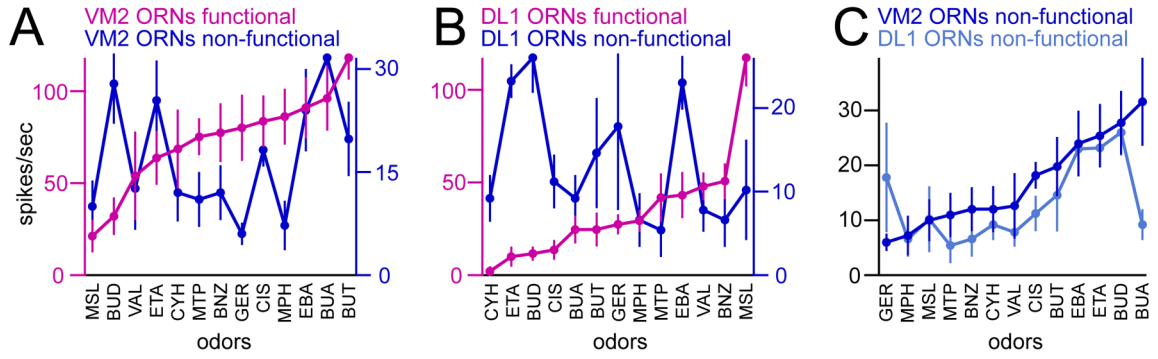
Figure 4. Odor tuning of PN responses postsynaptic to normal versus "silent" ORNs
(A–B) Tuning curves comparing odor responses of PNs postsynaptic to wild-type (magenta) and mutant ORNs (blue). PNs are postsynaptic to glomerulus VM2 (A) or DL1 (B). Each point represents firing rate over the 500-msec odor stimulus period, averaged across experiments (mean ± SEM). Note different *y*-scales for magenta and blue symbols. Odors are arranged so the smallest wild-type responses are on the left and the largest are on the right. See Methods for odor abbreviations.
(C) Tuning curves comparing odor responses of VM2 and DL1 PNs postsynaptic to mutant ORNs. Note correlated but not identical odor tuning.
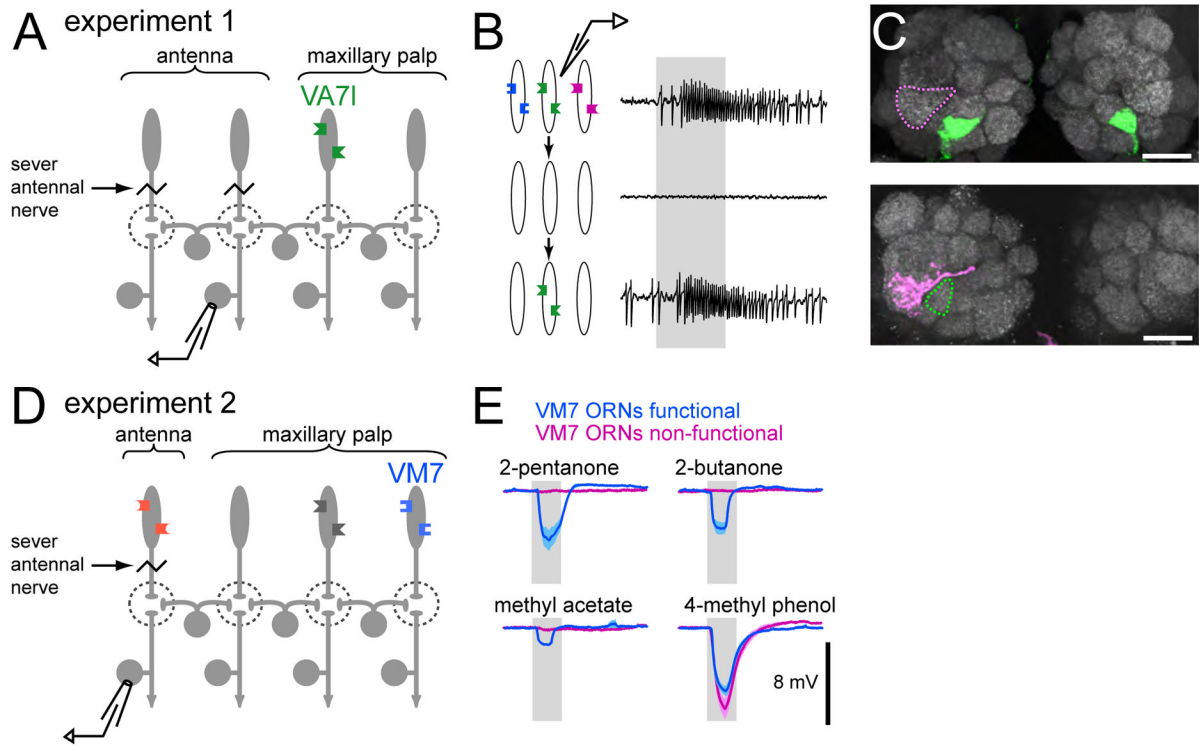
Figure 5. Two strategies for stimulating a single ORN type

(A) In experiment 1, only one maxillary palp ORN type (VA71) has functional odorant receptors. Antennal nerves are severed. Recordings are performed from PNs postsynaptic to antennal glomeruli.

(B) Genetic strategy to limit functional odor receptors to a single type of ORN. Top: single-sensillum recording from wild-type ORN projecting to glomerulus VA71. (The second ORN in this sensillum has been killed with diphtheria toxin to show only the VA71 ORN spikes; see Supplemental Table S1). Middle: in the $Or83b^2$ mutant, all spontaneous and odor-evoked activity is eliminated from maxillary palp ORNs. Bottom: odor response is rescued in VA71 ORNs by selective expression of Or83b in these neurons. Gray bar = 500 msec puff of methyl salicylate.

(C) Both ORNs and PNs show correct glomerular targeting in flies with "rescued" VA71 ORNs. Top: projection of a confocal stack through antennal lobes of a fly with rescued VA71 ORNs. VA71 ORNs are labeled with CD8:GFP (green). A neighboring glomerulus (VA1v) is outlined in magenta. Bottom: biocytin-fill of a VA1v PN (magenta) recorded in a fly with rescued VA71 ORNs where all other ORNs are non-functional. This PN does not invade glomerulus VA71 (green). Scale bars=20 μm.

(D) Experiment 2 uses a restricted odor set to selectively stimulate VM7 ORNs. Antennal nerves are severed, and the $\Delta85$ mutation is used to reduce ORN activity in two maxillary palp ORN types. Recordings are performed from PNs postsynaptic to antennal glomeruli.

(E) A restricted odor set activates only VM7 ORNs. Local field potential recordings from the maxillary palp of flies with either functional (blue; genotype $+/+;\Delta85$) or non-functional VM7 ORNs (magenta; genotype $Or42a^{f04305}; \Delta85$). Responses are only present when VM7 ORNs are functional. As a positive control, we confirmed that 4-methyl phenol elicits a robust response in both genotypes; this odor activates several maxillary palp ORNs that are functional in both genotypes. Traces are mean ± SEM, averaged across experiments (n=3 for each genotype).
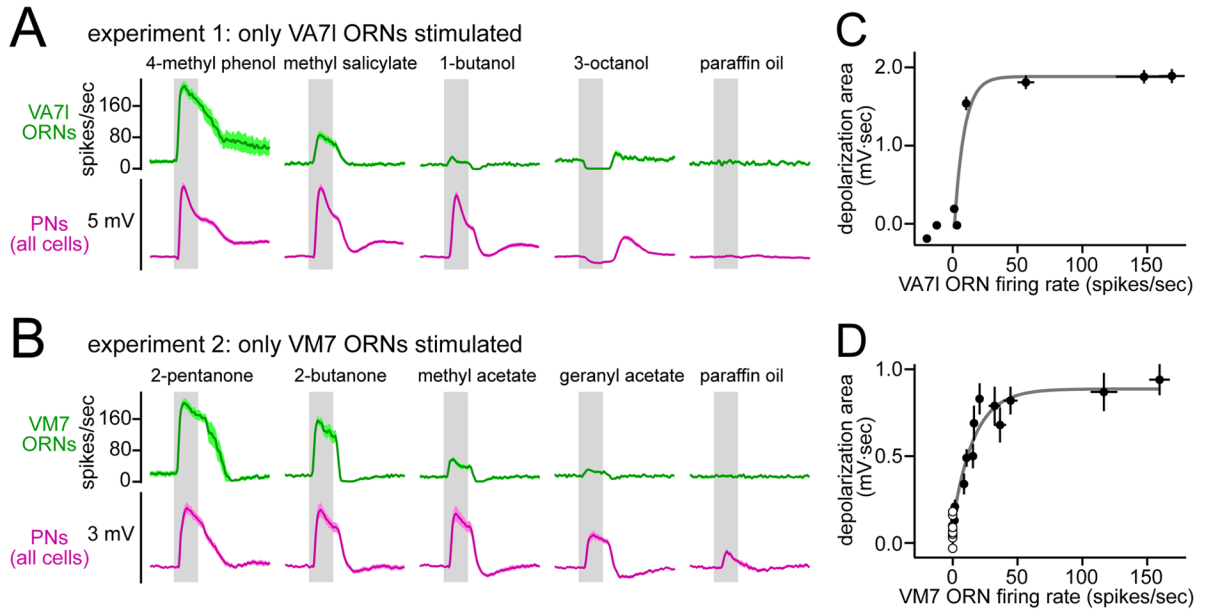
Figure 6. Odor stimulation of one ORN type evokes lateral input to many PNs
(A) Experiment 1. Top: peristimulus-time histograms show odor responses of VA71 ORNs (n=5). Bottom: average depolarizations recorded in PNs postsynaptic to glomeruli lacking direct ORN input (n=72).
(B) Experiment 2. Top: peristimulus-time histograms showing odor responses of VM7 ORNs (n=6). Bottom: average depolarizations recorded in PNs postsynaptic to glomeruli lacking direct ORN input (n=15).
(C) Experiment 1. Average depolarization area plotted versus VA71 ORN firing rate. Each point represents a different odor. Curve is an exponential fit (only excitatory ORN responses are included in fit).
(D) Experiment 2. Average depolarization area plotted versus VM7 ORN firing rate for each odor (solid symbols). Curve is an exponential fit. In flies lacking functional VM7 ORNs (open symbols), odor-evoked depolarizations are virtually absent ($Or42a^{f04305}$;$\Delta 85$; n=3).
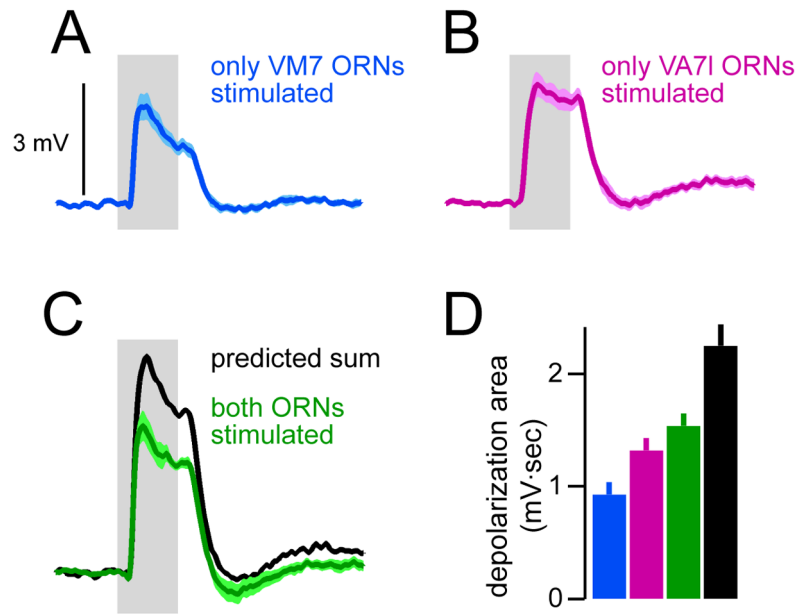All panels: values are mean ± SEM, averaged across experiments.

Figure 7. Lateral excitatory circuits sub-linearly summate inputs from multiple ORN types
(A) Average depolarization evoked in antennal PNs by selective stimulation of VM7 ORNs
with 2-butanone (10^{-5} dilution) in $\Delta 85$ flies.
(B) Average depolarization evoked in antennal PNs by selective stimulation of VA71 ORNs
with methyl salicylate (10^{-2} dilution) in $\Delta 85$ flies, recorded from the same PNs as in (A).
(C) Comparing the average depolarization evoked by simultaneous stimulation of both ORN
types (green), versus the predicted linear sum of stimulating each ORN type alone (black).
(D) Depolarization quantified as the area under the membrane potential deflection.
All panels: values are mean ± SEM, averaged across 8 PNs recorded in different flies. All PNs
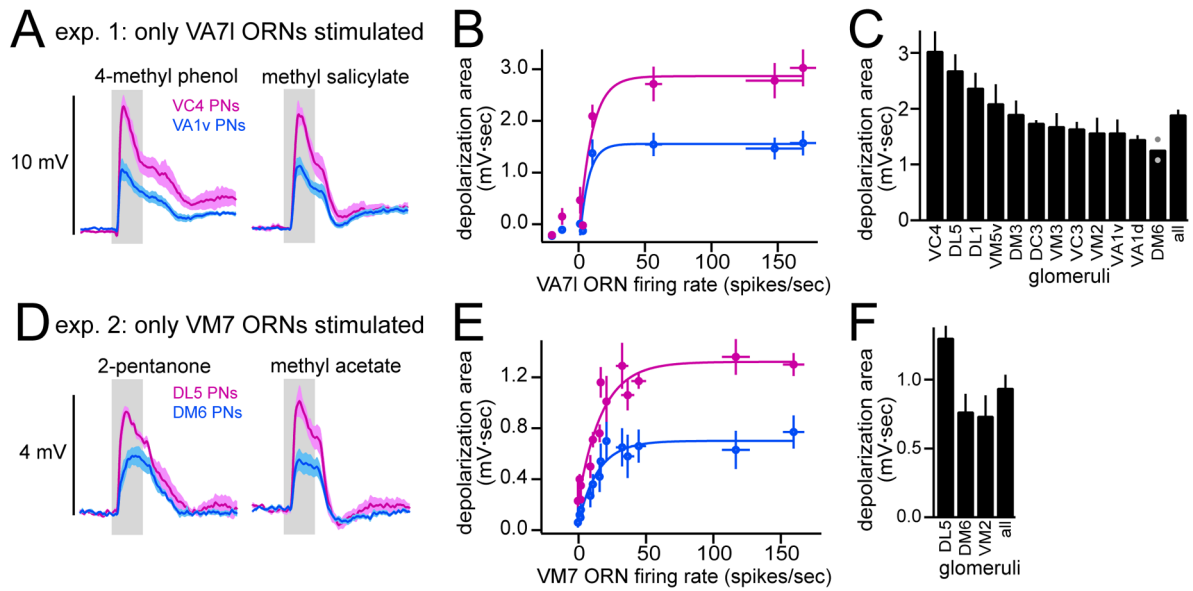were postsynaptic to glomeruli DL5, DM6, or VM2. Vertical scaling is the same in panels A–
C.

Figure 8. The strength of lateral connections is heterogeneous and stereotyped across flies
(A) Experiment 1: stimulation of VA71 ORNs evokes different levels of lateral depolarization in PNs postsynaptic to two different glomeruli (magenta=VC4, blue=VA1v).
(B) Depolarization area in these PNs is plotted versus VA71 ORN firing rate for each odor. Curves are exponential fits (only excitatory ORN responses are included in fit).
(C) Comparing lateral depolarization in all PN types that we recorded from at least 3 times (except DM6 where n = 2, gray dots). Graph shows average response to 4-methyl phenol in these PNs.
(D) Experiment 2: stimulation of VM7 ORNs evokes different levels of lateral depolarization in PNs postsynaptic to two different glomeruli (magenta=DL5, blue=DM6).
(E) Depolarization area in these PNs is plotted versus VM7 ORN firing rate for each odor. Curves are exponential fits.
(F) Comparing lateral depolarization area in three different glomeruli (n≥3 for each). Graph shows average response to 2-pentanone for each glomerulus.
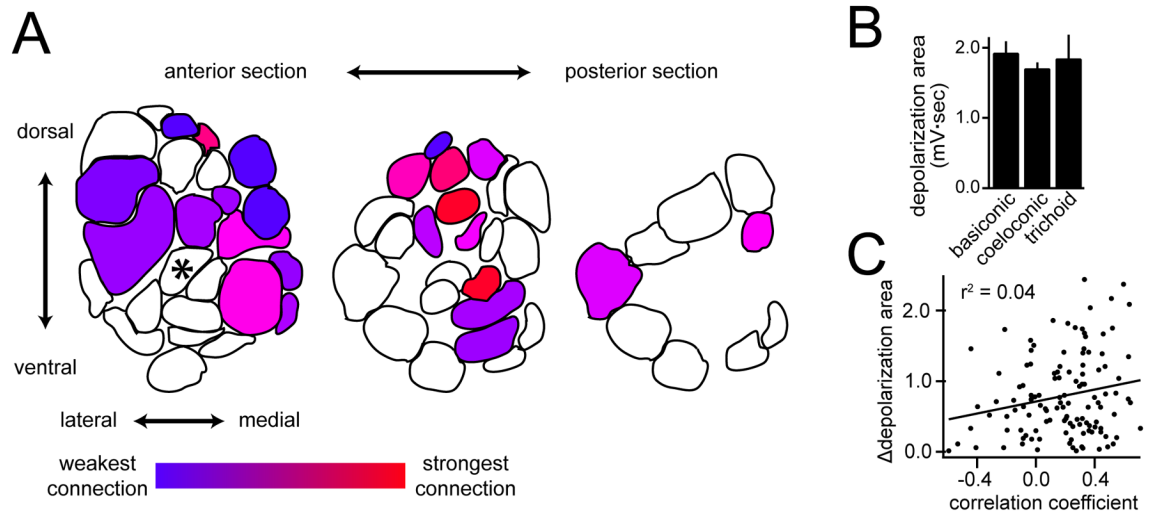All panels: values are mean ± SEM, averaged across experiments.

Figure 9. Lateral excitation is broadly distributed throughout the antennal lobe
(A) Schematic representation of all glomeruli in the antennal lobe, represented as three sections through the fly's right lobe (modified from Laissue et al., 1999). Color indicates average relative depolarization measured in PNs postsynaptic to each glomerulus during selective stimulation of VA71 ORNs. Asterisk marks glomerulus VA71. We did not sample PNs postsynaptic to white glomeruli.

(B) Glomeruli postsynaptic to different morphological types of sensilla receive similar levels of lateral input. Graph compares average depolarization area (± SEM) evoked by 4-methyl phenol in glomeruli targeted by ORNs in basiconic sensilla (n=14 glomeruli), coeloconic sensilla (n=3 glomeruli), and trichoid sensilla (n=6 glomeruli). Data on morphological types was taken from Couto et al. (2005).

(C) There is no relationship between odor tuning and strength of lateral input. Comprehensive odor tuning data for 16 ORN types was taken from Hallem and Carlson (2006). For every possible pair-wise combination of 16 glomeruli, the difference in the average lateral depolarization evoked by 4-methyl phenol in these two PN types is plotted versus the correlation between the odor tuning of the ORN inputs to those glomeruli.